**TECHNISCHE MECHANIK**
an open access journal

journal homepage: www.ovgu.de/techmech

Tech. Mech., Vol. 44, Is. 3, (2025), 194–200

Received: 16.10.2024
Accepted: 08.07.2025
Available online: 09.07.2025

# A Thermodynamic framework of Modeling Twinning-Induced Plasticity in Austenite-based Advanced High Strength Steels

Rashid Khan[1]*, Nashmi Hassan Alrasheedi[1], Aissa Rezzoug[2], Maaz Akhtar[3], Ali Khurshid Siddiqui[1], and Barun Haldar[3]

[1] Mechanical Engineering Department, College of Engineering, Imam Mohammad Ibn Saud Islamic University (IMSIU), Riyadh, Saudi Arabia
[2] Civil Engineering Department, College of Engineering, Imam Mohammad Ibn Saud Islamic University (IMSIU), Riyadh, Saudi Arabia
[3] Industrial Engineering Department, College of Engineering, Imam Mohammad Ibn Saud Islamic University (IMSIU), Riyadh, Saudi Arabia

**Abstract:** Advanced materials are widely recognized as a key enabler of technologies underpinning the Fourth Industrial Revolution (4IR), as progress in many sectors relies heavily on the availability of functionally graded and high-performance materials. In particular, the development of advanced metallic materials has made it possible to manufacture products and systems with complex geometries and tailored properties. Among these materials, Twinning-Induced Plasticity (TWIP) steels are prominent representatives of third-generation advanced high-strength steels (AHSS). Their superior mechanical properties arise from a combination of factors, including chemical composition, phase volume fractions, intricate microstructure, and the activation of mechanical twinning. This study focuses on modeling the deformation behavior of austenite-based TWIP steels using a combination of crystal plasticity and thermodynamic frameworks. Initially, mechanical twinning is integrated into a slip-based plasticity model. A thermodynamic approach is then developed to estimate the dissipated energy and Helmholtz free energy associated with both slip and twinning mechanisms. A numerical integration scheme is formulated and implemented in ABAQUS through a User-defined MATerial (UMAT) subroutine. Finite element models are constructed to predict the elastic-plastic and twinning responses of single- and polycrystalline austenite under biaxial loading conditions. The results reveal a significant variation in stress magnitude, particularly in polycrystalline austenite, when twinning is incorporated into the slip mechanism. This highlights the critical role of mechanical twinning in enhancing both the strength and formability of advanced high-strength steels.

**Keywords:** Crystallographic slip, Mechanical twinning, Crystal plasticity theory, Numerical modeling, Finite element simulations, Stress analysis

## 1 Preamble

Advanced materials play a crucial role in modern technological advancements, enabling the formation of a wide range of products across various industries. In parallel, the growth of advanced manufacturing techniques facilitates the development of such sophisticated products that are capable of withstanding challenging operating conditions. Specifically, Advanced High Strength Steels (AHSS) successfully addressed the challenges primarily related to the simultaneous improvements in both tensile strength and ductility. This historically unsolved hurdle overcomes, to the greater extent, by regulating microstructure, phase composition, and alloying elements in AHSS. Among other options, Twinning-Induced Plasticity (TWIP) steels stand out due to their exceptional strain hardening, ductility, and ultimate tensile strength. These exceptional qualities make them a prominent candidate in automotive, die manufacturing, and oil/gas sectors.

TWIP steels are primarily austenitic, characterized by Face Centered Cubic (FCC) structure with high Manganese (Mn) content, > 20% by weight. As a consequence, they normally exhibit low stacking fault energy (SFE) in the range of 20 to 40 mJ/m$^2$ under ambient conditions. This characteristic greatly contributing to their high-strain or work hardening capability. The significant strain hardening in TWIP steels arises from an increased volume fraction of twinned regions, which reduces the dislocation mean free path. Twinned regions act as barriers to dislocation glide, thereby enhancing strain-hardening effects Asgari et al. (1997); Bouaziz et al. (2011). This high work hardening rate is the key for achieving both high strength and ductility. On the other side, there are notable challenges with TWIP steels which are required be addressed. These mainly include complex thermomechanical milling process, high alloying cost, production of TWIP grades, poor weldability, and formation of manganese and aluminum oxides (MnO and $Al_2O_3$) Cooman et al. (2018).

Mechanical twinning, alongside slip, represents another form of inelastic deformation observed in metals, non-metals, and metallic glasses Fan et al. (2017). The occurrence of mechanical twinning is generally influenced by alloy's chemical composition, presence of retained austenite phase, and external conditions Pierce et al. (2014); Fei et al. (2014). In addition, stacking fault energy (SFE) of an alloy also plays key role in an activation of twinning Curtze et al. (2011); Idrissi et al. (2009); Cooman et al. (2018). Mechanical twinning can become more probable when SFE ranges between 20 and 40 mJ/m$^2$, often coexisting with dislocation glide. In contrast, when it drops below 20 mJ/m$^2$, a thermal martensitic transformation mechanism becomes secondary deformation

* E-mail address: rakhan@imamu.edu.sa
doi: 10.24352/UB.OVGU-2024-066

mode, along with dislocation glide Allain et al. (2004); Bhattacharyya and Weng (1994). However, in steel alloys with SFE values exceeding 45 mJ/m$^2$, both mechanical twinning and martensitic transformation become less energetically feasible, and crystallographic slip predominantly governs inelastic behavior Allain et al. (2004).

An integration of mechanical twinning in crystal plasticity theory, alongside crystallographic slip, is an important domain of research, especially in case of TWIP steels Tomé et al. (1991); Kalidindi (1998). Many researchers have extensively explored this area and established significant outcomes which help in understanding the deformation of behavior of TWIP steels. For instance, Van Houtte Houtte (1978) introduced a statistical method based on the volume fraction of twinned regions within grains and polycrystalline aggregates. This approach determines whether an entire grain reorient to a dominant twin orientation, maintaining total number of grain orientations by applying an "on or off" condition. Tome et al. Tomé et al. (1991) introduced a solution that utilized weighted grain orientations, allowing twinned regions to be reoriented at each time step without creating new orientations. Lebensohn and Tome Lebensohn and Tomé (1994) extended this approach by proposing methods for reorienting twin regions and calculating volume fractions in Taylor-type and self-consistent viscoplastic scheme. Kalidindi Kalidindi (1998) proposed an alternative framework for incorporating mechanical twinning in crystal plasticity theory. This model utilized the interpretation of Asaro and Rice Asaro and Rice (1977), where total deformation gradient is divided into elastic and plastic components through multiplicative decomposition. The plastic deformation gradient is further defined based on slip and mechanical twinning, and strain hardening effects are incorporated accordingly. Furthermore, the rate of change of twin volume fraction is assumed to depend on the resolved shear stress on active twin systems and their resistances against twinning, similar to the hardening behavior of slip systems Asaro and Rice (1977). The kinematic part of the proposed model is based on the formulation presented by Kalidindi (1998).

## 2 Twinning-Induced Plasticity: An energy-based model

In the present model, thermodynamic or energy-based approach is used for modeling deformation behavior of Austenitic Advanced High Strength Steels (AAHSS), where plasticity mainly happens due to crystallographic slip and mechanical twinning. In the preceding section, initially, a constitutive formulation of a non-recoverable, dissipated, part of energy is established. This is mainly based on the assumption that the dissipated energy is due to: $(i)$ rate of change of external mechanical work, $(ii)$ rate of change of enthalpy due to thermal load, $(iii)$ variation rate of internal energy, and $(iv)$ heat flux leaving the body. Furthermore, constitutive equations for a recoverable part of energy, Helmholtz free energy (HFE), are formulated based on the hypothesis that it consists of: $(i)$ rate of change of external mechanical work, $(ii)$ rate of variation of thermal load, $(iii)$ internal energy due to crystal defects, and $(iv)$ surface energy due to the formation of new surfaces as a result of twinning. The presented work is primarily based on the constitutive model proposed by Khan and Alfozan (2019); Khan et al. (2022).

### 2.1 Non-recoverable or dissipated energy

For a material point of infinitesimal volume, $dv$ belongs to a region, $R$, subjected to an external thermomechanical load, the specific dissipated energy (energy per unit volume) can be expressed in the form of entropy as:

$$\dot{e}_d = \dot{\Upsilon}\, T\,, \tag{1}$$

where $\dot{\Upsilon}$ is the rate of variation of the entropy and $T$ is an absolute temperature. By adopting the principle of Clausius-Duhem inequality, rate of change of entropy can be stated as:

$$\dot{\Upsilon} = \dot{\Upsilon}_e - \dot{\Upsilon}_i\ . \tag{2}$$

Here, $\dot{\Upsilon}_e$ and $\dot{\Upsilon}_i$ are the rate of change of entropy due to an external thermomechanical load and the rate of internal entropy generation, respectively. Equation (2) can also be expressed in the form of heat generation as:

$$\dot{\Upsilon} = \rho_0 \dot{\Upsilon}_e - \left(\frac{Q_i}{T}\right)\,, \tag{3}$$

where, $\rho_o$ represents material density in initial state, and $Q_i$ is an internal heat generation per volume. In Eq.(3), volumetric heat generation can be estimated through the energy conservation principle and expressed as:

$$Q_i = \rho_0 \dot{e}_m - \boldsymbol{\sigma}\dot{\mathbf{D}} + \nabla\vec{\mathbf{h}_\mathbf{f}}\ . \tag{4}$$

Here, $\dot{e}_m$ is the rate of internal energy per unit mass, $D$ is the total deformation gradient, $\nabla$ is the divergence operator, and $\vec{\mathbf{h}_\mathbf{f}}$ is the heat flux. After the substitution of Eq.(4) in (3) and then in (1) provides:

$$\dot{e}_d = \boldsymbol{\sigma}\mathbf{D} + \rho_0 T\dot{\Upsilon}_e - \rho_0\dot{e}_m - \nabla\vec{\mathbf{h}_\mathbf{f}}\ . \tag{5}$$

A non-recoverable part of energy, as shown by Eq.(5), consists of (in sequential order on the right side of equation) energy due to mechanical work per unit volume, thermal energy as a result of enthalpy variation, internal energy generation per unit volume, and the heat flux leaving the body surface per unit area. The constitutive equations of all these terms are derived in detail by Khan and Alfozan (2019). For simplification, the final form of the dissipated energy equation is presented by Eq.() as:

$$\dot{e}_d = \sum_{\alpha=1}^{\zeta_s} \vartheta^{\alpha}\left(\tau^{\alpha} + \chi^{\alpha} - \rho_0 \frac{\partial e_m}{\partial \xi}\Psi^{\alpha}\right)\dot{\gamma}^{\alpha} + \sum_{\beta=1}^{\zeta_t} \vartheta^{\beta}\left(\tau^{\beta} + \chi^{\beta} - \rho_0 \frac{\partial e_m}{\partial \xi}\Psi^{\beta}\right)\dot{\gamma}^{\beta} - (T)\nabla \Upsilon_f \ . \tag{6}$$

where, $\zeta_s$ and $\zeta_t$ are the number of active slip and twin systems, respectively, $\vartheta^{\alpha}$ and $\vartheta^{\beta}$ are the volume fractions of slip and twin systems, respectively, $\tau^{\alpha}$ and $\tau^{\beta}$ are the resolved shear stresses on $\alpha$-slip and $\beta$-twin systems, respectively, $\chi^{\alpha}$ and $\chi^{\beta}$ are respectively the thermal equivalents of the resolved shear stress and represent the contribution of heat energy to slip and twin activities, $\xi$ is the crystal defect microstrain parameter that is the measure of energy required to overcome localized strain, $\Psi^{\alpha}$ and $\Psi^{\beta}$ are stress-equivalent parameters, depends on slip and twin resistances of $\alpha$ and $\beta$ systems, $\dot{\gamma}^{\alpha}$ and $\dot{\gamma}^{\beta}$ are shear strain rates of $\alpha$ and $\beta$ systems, respectively, and $\Upsilon_f$ is the entropy flux due to heat flux $h_f$.

### 2.2 Recoverable or Helmholtz free energy (HFE)

In the present model, a recoverable part of energy, mainly due to elastic deformation, is assumed to be a function of mechanical and thermal loads, microstrain due to crystallographic defects, and surface energy. Therefore, HFE can be expressed as a function of four state variables i.e. elastic deformation gradient $\mathbf{D}^e$, absolute temperature $T$, crystal defect microstrain parameter $\xi$, and twin martensite volume fraction $\upsilon$. In the current work, it is assumed that all the constituents of HFE are independent to each other. Therefore, an additive decomposition is used as follows:

$$e_H = e_{Hm}(\mathbf{D}^e) + e_{Ht}(T) + e_{Hd}(\xi) + e_{Hs}(\upsilon) \ , \tag{7}$$

where the mechanical, thermal, crystal defect, and surface energy part are respectively represented by $e_{Hm}$, $e_{Ht}$, $e_{Hd}$, and $e_{Hs}$. The mechanical contribution of HFE depends on the Green finite strain tensor, $\widetilde{\mathbf{E}}^e$ and the twinned martensite volume fraction, $\vartheta^{\beta}$, and can be expressed as:

$$e_{Hm}(\widetilde{\mathbf{E}}^e, \vartheta^{\beta}) = \frac{1}{\rho_0}\left\{(\mathbf{D}^e\mathbf{D}^p) : (\widetilde{\mathbb{C}}^e : \widetilde{\mathbf{E}}^e\widetilde{\mathbf{E}}^e)\right\}(\mathbf{D}^p)^T : \left[\mathbf{R}^e + (\mathbf{R}^e)^T\right]^{-1} \ . \tag{8}$$

Here, $\mathbf{D}^e$ and $\mathbf{D}^p$ are elastic and plastic deformation gradients, respectively, $\widetilde{\mathbb{C}}^e$ is the equivalent elasticity tensor (combination of material properties for austenite and martensite), and $\mathbf{R}^e$ is the symmetric part of elastic velocity gradient. It is evident from Eq.() that $e_{Hm}$ is a function of volume fraction of twinned region, $\vartheta^{\beta}$ which changes throughout the deformation. The thermal contribution of HFE is extracted using the constitutive relation between the entropy density and temperature and can be expressed in the final form as:

$$e_{Ht} = T\left[ - h_e \ln\left(\frac{T}{T_r}\right) + \left(h_e - \Upsilon^e_{m,0}\right)\right] \ , \tag{9}$$

where, $h_e$ is an effective specific heat, $T_r$ is the room temperature, $\Upsilon^e_{m,0}$ is the entropy. An effective specific heat can be estimated by the volume fractions of slip and twinned regions as:

$$h_e = \sum_{\alpha=1}^{\zeta_s} \vartheta^{\alpha} h_s + \sum_{\beta=1}^{\zeta_t} \vartheta^{\beta} h_t \ . \tag{10}$$

In Eq.(10), $h_s$ and $h_t$ are, respectively the specific heats of slip and twinned regions. Furthermore, it is evident that specific heat of a crystal evolves with the volume fraction of twinned region. The crystal defect energy contribution of HFE can be approximated as a function of equivalent modulus of rigidity, $G_e$ and crystal defect microstrain parameter, $\xi$ as:

$$e_{Hd}(\xi) = \frac{1}{2\rho_0}\varphi G^e \xi^2 \ , \tag{11}$$

where, $\varphi$ is a dislocation interaction parameter that includes the effects of dislocations mobility and defects' interactions. The surface energy contribution of HFE is considered to be dependent on the geometry and dispersal of martensite plates in an austenite phase. Crystal defect microstrain parameter accounts the effects of microstrain that develops around or within the crystal due to interatomic defects. Its magnitude depends on slip resistance, dislocation interaction factor, and modulus of rigidity. Moreover, an interfacial area of austenite and martensite is a linear function of martensite volume fraction. In this case, surface energy can be stated as:

$$e_{Hs}(\vartheta) = \frac{e_i^{\beta}}{\rho_0 l_0} \sum_{\alpha=1}^{\zeta_s} \vartheta^{\alpha} \left(1 - \sum_{\alpha=1}^{\zeta_s} \vartheta^{\alpha}\right) . \tag{12}$$

Here, $e_i^{\beta}$ is the interfacial energy per unit area for $\beta$-twin system, $l_0$ is the length scale parameter which is the ratio of volume and surface area of martensite plate; considered as circular in spherical austenite phase domain. Substitution of Eqs.(2.2), (9), (11), and (12) in (7) provides final form of Helmholtz free energy as:

$$\begin{aligned} e_H =& \frac{1}{\rho_0}\left\{(\mathbf{D}^e\mathbf{D}^p) : (\widetilde{\mathbb{C}}^e : \widetilde{\mathbf{E}}^e\widetilde{\mathbf{E}}^e)\right\}(\mathbf{D}^p)^T : \left[\mathbf{R}^e + (\mathbf{R}^e)^T\right]^{-1} T\left[ - h_e \ln\left(\frac{T}{T_r}\right) + \left(h_e - \Upsilon^e_{m,0}\right)\right] + \frac{1}{2\rho_0}\varphi G^e \xi^2 + \\ & \frac{e_i^{\beta}}{\rho_0 l_0} \sum_{\alpha=1}^{\zeta_s} \vartheta^{\alpha} \left(1 - \sum_{\alpha=1}^{\zeta_s} \vartheta^{\alpha}\right) . \end{aligned} \tag{13}$$

The constitutive formulation of parameters $\tau^{\alpha}$, $\tau^{\beta}$, $\mathbf{D}^e$, $\mathbf{D}^p$, and $\mathbf{R}^e$ is comprehensively discussed in Khan and Alfozan (2019) through the kinematic decomposition of material point in three intermediate configurations. This constitutive development can be utilized in Eqs.(6 and 13) to estimate dissipated and Helmholtz free energies of a material point in austenite-based Advanced High Strength Steels subjected to thermomechanical load. In the succeeding section, an implementation of the developed constitutive model is presented by simulating the deformation behavior of austenite-based material subjected to biaxial loading condition.

## 3 Finite Element Modeling and Simulations

In finite element simulations, deformation pattern of single and multigrains austenite-based material, subjected to biaxial tension, is predicted. For single crystal, crystallographic directions [100], [110], and [111], are selected, while multigrain austenite is assumed to have 500 randomly oriented grains. A detailed number of grains independent study is reported in Khan and Alfozan (2019), where the authors concluded that no significant variation in results is observed beyond 500 grains. The random texture is incorporated using single eight-node 3D brick element with reduced integration (C3D8R). The orientations of grains are defined in the form of Euler angles based on Kocks convention Kocks (1988).

The material parameters of austenite phase are taken as reported by Turteltaub and Suiker (2006). The material tensor components are defined by Furnémont et al. (2002) as: $E^a_{11}$ = 286.6, $E^a_{12}$ = 166.4, and $E^a_{44}$ = 145.0 in GPa. These were estimated by nano-indentation experiments on transformation-induced plasticity steel with 0.92 wt% of austenitic phase along with other phases like ferrite, bainite, and some traces of martensite. Furthermore, modulus of rigidity $G^a$ and bulk modulus $K^a$ are defined through isotropic equations described for cubic crystals as reported in Khan and Alfozan (2019). Thus, their values are obtained as $G^a$ = 111.0 GPa and $K^a$ = 206.5 GPa. The modulus of rigidity of twinned martensite is considered as $G^t$ = 98.4 GPa, reported by Tjahjanto (2007). The initial value of crystal defect microstrain parameter, $\xi_0$ is taken as $4.5x10^{-4}$, as described in Khan and Alfozan (2019). The density of austenite is considered the same as that of carbon steel, i.e. $\rho_0 = 7.8\,\mathrm{x}\,10^{-6}$ kg / mm$^3$. The details of other parameters can be referred from Khan et al. (2016); Khan and Alfozan (2019).

## 4 Results and discussion

The energy-based Twinning-Induced Plasticity (TWIP) model was validated against experimental data reported in Khan and Alfozan (2019), where a sensitivity analysis of the model parameters was conducted to minimize prediction errors. The simulation results demonstrated strong agreement with the experimental observations, confirming the model's reliability and accuracy.

The equivalent stress-strain variation of single and multigrain austenite steel is represented in Figure 1. A notable difference is observed in crystallographic direction [111] and multigrain, however; almost none in [100] and [110]. In addition, the material point loaded in the [111] direction shows the highest magnitude of stress (~ 700 MPa at the equivalent strain 0.4) among all crystallographic orientations. Besides, [100] and [110] have a similar level of stress, ~ 535 MPa, at 0.40 equivalent strain. Multigrain austenite demonstrates similar deformation behavior, however; with larger magnitude of stress as single grain. This indicates that the interaction among slip-slip and slip-twin systems becomes dominant, which may enhance the overall hardening exponent.

Activation of slip and twin planes, quantify the respective contributions to plastic strain, can be traced by slip and twin shear strains, as illustrated by Figures 2 and 3, respectively. A general observation for all directions is that slip contribution is far more than twin (> 10 times). Secondly, for the crystallographic direction [111], the magnitude of slip shear strain is higher than other two directions, however; the reverse is seen in case of twinning shear strain. This indicates that the mechanical twinning contribution to overall inelastic deformation is much lesser in case of [111] direction.

The dissipated and Helmholtz free energies are also estimated for three crystallographic directions, as shown in Figures 4 and 5, respectively. The dissipated energy variation with respect to equivalent strain follows similar trend for all directions. However; its magnitude, 0.96 J/mm$^3$ at 0.54 equivalent strain, for [111] is significantly higher than others two, as shown in Figure 4. This

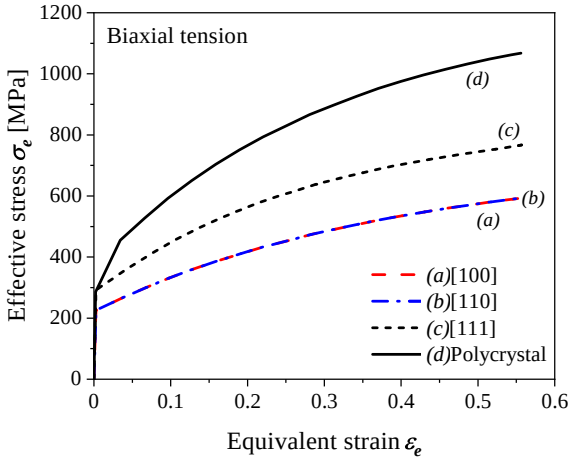


Fig. 1: Deformation behavior of single and polycrystalline austenite under biaxial loading

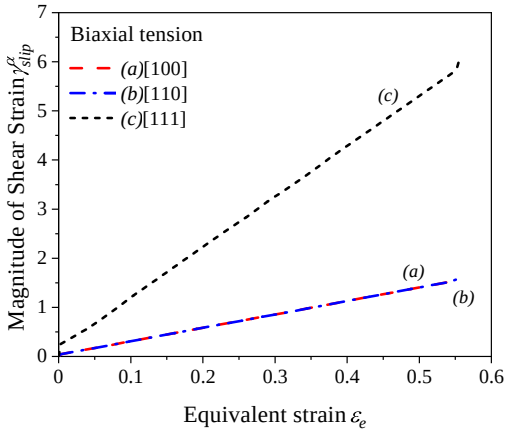


Fig. 2: Combined shear strain variation of active slip planes, $\gamma^{\alpha}$ in biaxial tension for [100], [110], and [111] directions

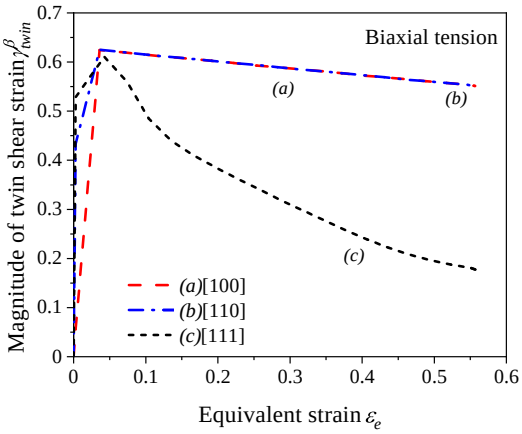


Fig. 3: Combined shear strain variation of active twin planes, $\gamma^{\beta}$ in biaxial tension for [100], [110], and [111] directions

behavior is inline with the shear strain variation for slip deformation, as illustrated in Figure 2, where shear strain magnitude due to slip is highest for [111] direction. Helmholtz free energy (HFE) variation with equivalent strain, as shown in Figure 5, follows similar trend as dissipated energy, where crystallographic direction [111] has significant difference than other two. It has higher magnitude at lower strain, -1.193343 J/mm$^3$, and gradually decreases at higher values. However, for [100] and [110] directions, a constant value, -1.1934 J/mm$^3$, is observed.

## 5 Conclusions

A deformation behavior of an austenitic advanced high strength TWIP steel is modeled by integrating thermodynamic-based scheme into crystal plasticity theory. In this, two primary modes of inelastic deformation, crystallographic slip and mechanical twinning, are incorporated. The constitutive model is numerically solved through finite element theory using a User-MATerial (UMAT) subroutine in ABAQUS software. As a test case, the deformation behaviors of single and multigrain material points

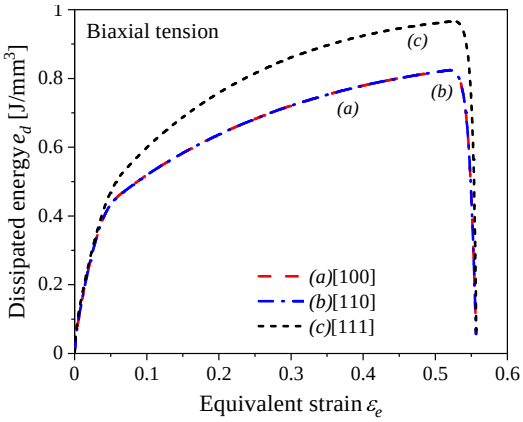


Fig. 4: Dissipated energy variation in biaxial tension for three crystallographic [100], [110], and [111] directions

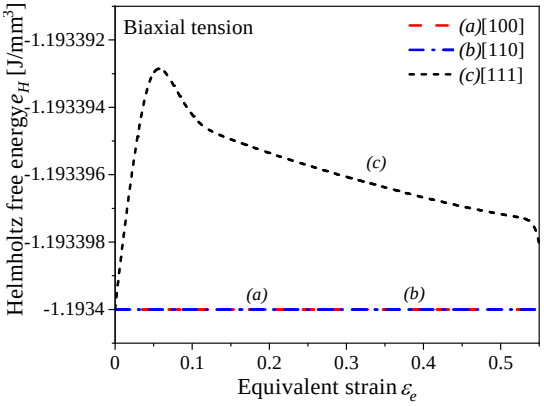


Fig. 5: Helmholtz free energy variation in biaxial tension for three crystallographic [100], [110], and [111] directions

subjected to biaxial loading condition are simulated. A prominent variation in the magnitude of equivalent stress is observed for direction [111] and multigrain, and negligible in [100] and [110]. Furthermore, a material point loaded in [111] direction shows highest magnitude of stress (~ 700 MPa at the equivalent strain 0.4) among all crystallographic orientations. Based on the results of shear strain rates, it is found that the contribution of slip is far more than mechanical twining for [111] direction as others. It is also observed that the magnitudes of non-recoverable (dissipated) and recoverable (Helmholtz) energies are comparatively higher for [111] direction at the same equivalent strain. Finally, it can be concluded that the presented thermodynamic-based model may provide an opportunity to observe the deformation behavior of austenite-based TWIP steels once subjected to thermomechanical loads. This may helps in implementing TWIP steels in a range of applications where contradictory material properties, formability and strength, are desirable.

## References

S. Allain, J.-P. Chateau, O. Bouaziz, S. Migot, and N. Guelton. Correlations between the calculated stacking fault energy and the plasticity mechanisms in Fe-Mn-C alloys. *Materials Science and Engineering: A*, 387-389:158–162, 2004. doi: https://doi.org/10.1016/j.msea.2004.01.059 http://www.sciencedirect.com/science/article/pii/S0921509304004356.

R. J. Asaro and J. R. Rice. Strain localization in ductile single crystals. *Journal of the Mechanics and Physics of Solids*, 25(5): 309–338, 1977.

S. Asgari, E. El-Danaf, S. R. Kalidindi, and R. D. Doherty. Strain hardening regimes and microstructural evolution during large strain compression of low stacking fault energy fcc alloys that form deformation twins. *Metallurgical and Materials Transactions A*, 28(9):1781–1795, 1997.

A. Bhattacharyya and G. J. Weng. An energy criterion for the stress-induced martensitic transformation in a ductile system. *Journal of the Mechanics and Physics of Solids*, 42(11):1699–1724, 1994.

O. Bouaziz, S. Allain, C. P. Scott, P. Cugy, and D. Barbier. High manganese austenitic twinning induced plasticity steels: A review of the microstructure properties relationships. *Current Opinion in Solid State and Materials Science*, 15(4):141–168, 2011.

Bruno C. De Cooman, Yuri Estrin, and Sung Kyu Kim. Twinning-induced plasticity (TWIP) steels. *Acta Materialia*, 142:283–362, 2018. doi: https://doi.org/10.1016/j.actamat.2017.06.046 http://www.sciencedirect.com/science/article/pii/S1359645417305219.

S. Curtze, V.-T. Kuokkala, A. Oikari, J. Talonen, and H. Hänninen. Thermodynamic modeling of the stacking fault energy of austenitic steels. *Acta Materialia*, 59(3):1068–1076, 2011. doi: https://doi.org/10.1016/j.actamat.2010.10.037 http://www.sciencedirect.com/science/article/pii/S1359645410007007.

J. Fan, J. W. Qiao, Z. H. Wang, W. Rao, and G. Z. Kang. Twinning-induced plasticity (TWIP) and work hardening in Ti-based metallic glass matrix composites. *Scientific Reports*, 7(1):1877, 2017. doi: https://doi.org/10.1038/s41598-017-02100-9.

L. Fei, Z. Weigang, and D. Wenjiao. Stress-strain Response for Twinning-induced Plasticity Steel with Temperature. *Procedia Engineering*, 81:1330 – 1335, 2014. ISSN 1877-7058. doi: https://doi.org/10.1016/j.proeng.2014.10.152 http://www.sciencedirect.com/science/article/pii/S1877705814014313. 11th International Conference on Technology of Plasticity, ICTP 2014, 19-24 October 2014, Nagoya Congress Center, Nagoya, Japan.

Q. Furnémont, M. Kempf, P. J. Jacques, M. Göken, and F. Delannay. On the measurement of the nanohardness of the constitutive phases of TRIP-assisted multiphase steels. *Materials Science and Engineering: A*, 328(1-2):26–32, 2002.

P. V. Houtte. Simulation of the rolling and shear texture of brass by the Taylor theory adapted for mechanical twinning. *Acta Metallurgica*, 26:591–604, 1978.

H. Idrissi, L. Ryelandt, M. Veron, D. Schryvers, and P.J. Jacques. Is there a relationship between the stacking fault character and the activated mode of plasticity of fe-mn-based austenitic steels? *Scripta Materialia*, 60(11):941–944, 2009. doi: http://dx.doi.org/10.1016/j.scriptamat.2009.01.040.

Surya R. Kalidindi. Incorporation of deformation twinning in crystal plasticity models. *Journal of the Mechanics and Physics of Solids*, 46(2):267–290, 1998.

Rashid Khan and Adel Alfozan. Modeling of twinning-induced plasticity using crystal plasticity and thermodynamic framework. *Acta Mechanica*, 230(8):2687–2715, August 2019.

Rashid Khan, Tasneem Pervez, and Sayyad Zahid Qamar. Modeling and simulations of transformation and twinning induced plasticity in advanced high strength austenitic steels. *Mechanics of Materials*, 95:83–101, 2016.

Rashid Khan, Pervez Tasneem, Alfozan Adel, Qamar Sayyad, Zahid, and Mohsin Sumiya. Numerical modeling and simulations of twinning−induced plasticity using crystal plasticity finite element method. *Crystal*, 2022.

U. F. Kocks. A symmetric set of euler angles and oblique orientation space section. In J. S. Kallend and G. Gottstein, editors, *Eight International Conference on Textures of Materials*, volume 2, pages 31–36, Warrendale, PA: The Metallurgical Society, 1988.

R.A. Lebensohn and C.N. Tomé. A self-consistent viscoplastic model: prediction of rolling textures of anisotropic polycrystals. *Materials Science and Engineering: A*, 175(1):71 – 82, 1994. ISSN 0921-5093. doi: https://doi.org/10.1016/0921-5093(94)91047-2 http://www.sciencedirect.com/science/article/pii/0921509394910472. NATO Advanced Research Workshop on Polyphase Polycrystal Plasticity.

D.T. Pierce, J.A. Jiménez, J. Bentley, D. Raabe, C. Oskay, and J.E. Wittig. The influence of manganese content on the stacking fault and austenite-$\epsilon$ martensite interfacial energies in Fe-Mn-(Al-Si steels investigated by experiment and theory. *Acta Materialia*, 68:238–253, 2014. ISSN 1359-6454. doi: https://doi.org/10.1016/j.actamat.2014.01.001 http://www.sciencedirect.com/science/article/pii/S135964541400010X.

D. D. Tjahjanto. *Micromechanical modeling and simulations of transformation-induced plasticity in multiphase steels*. PhD thesis, Faculty of Aerospace Engineering, University of Delft, Netherlands, 2007.

C. N. Tomé, R. A. Lebensohn, and U. F. Kocks. A model for texture development dominated by deformation twinning: Application to zirconium alloys. *Acta Metallurgica et Materialia*, 39:2667–2680, 1991.

S. Turteltaub and A. S. J. Suiker. A multiscale thermomechanical model for cubic to tetragonal martensitic phase transformations. *International Journal of Solids and Structures*, 43(14-15):4509–4545, 2006.